Eighth South African Conference on Computational and Applied Mechanics
SACAM2012
Johannesburg, South Africa, 3−5 September 2012
©SACAM

Tutorial on state variable based plasticity: An Abaqus UHARD subroutine.

G. J. Jansen van Rensburg and S. Kok
Mathematical Modelling, CSIR Modelling and Digital Science
P.O. Box 395, Pretoria, 0001
jjvrensburg@csir.co.za

***Abstract*—Since plasticity is path dependent, it is necessary to properly take into account the deformation, strain rate and temperature history in applications such as crash worthiness and ballistics simulations. To accurately model the evolution of the yield stress, the incremental (differential) update from a previous converged time step is required instead of a closed form expression that relates flow stress to plastic strain. Elasto-viscoplastic models that make use of state variables better capture the physical phenomenon of a perceived lag between a change in strain rate or temperature and the subsequent stress response. It is impossible to capture this when making use of a closed form expression or data table based method. One model that makes use of an evolving state variable is the Mechanical Threshold Stress (MTS) model. In this paper, the implementation of the MTS model into an Abaqus user hardening (UHARD) subroutine is discussed and the code is included. The aim is not to improve on the current knowledge of the model, but to illustrate the ease with which a state variable based plasticity model can be implemented and used instead of an empirical (closed form expression) or data table based method. The MTS model is compared to the Johnson-Cook plasticity model which takes the form of a simple closed form expression relating yield stress to plastic strain as a function of temperature and strain rate. The model parameters are calibrated using isothermal, constant strain rate experimental data and then used to predict the stress response for a strain rate jump test and a temperature change test.**

***Keywords*—Mechanical Threshold Stress (MTS); Plasticity; Abaqus User Subroutines; UHARD**

INTRODUCTION

The Mechanical Threshold Stress (MTS) model [2] was developed to describe the post yielding behaviour of metals. It has demonstrated the ability to accurately model the effect of temperature and plastic strain rate on the post yielding behaviour of metals.

In this paper, the MTS model is calibrated using isothermal, constant strain rate data on OFHC Cu digitised from the Ph.D. thesis by A.B. Tanner [6] as an example. The model is then used to predict a strain rate jump test and temperature change test. Data for these experimental tests are also available in [6]. The Johnson-Cook plasticity model [3] is calibrated on the same data and also used to predict the strain rate jump and temparature change response for comparison.

This paper provides a tutorial on the MTS model and its implementation into an Abaqus environment. The code of the Abaqus user subroutine is included at the end of the article.

I. THEORY

In the MTS model, a material has a theoretical maximum flow stress at 0 K, called the mechanical threshold, $\hat{\sigma}$. The material flow stress, σ_y, is obtained by scaling the mechanical threshold to accommodate rate and temperature dependence.

Firstly, the threshold flow stress can be separated into an athermal component $\hat{\sigma}_a$ and thermal components $\hat{\sigma}_t^\kappa$.

$$\hat{\sigma} = \hat{\sigma}_a + \sum_\kappa \hat{\sigma}_t^\kappa. \tag{1}$$

The athermal component $\hat{\sigma}_a$ characterises the rate-independent interactions of dislocations with long-range barriers. The thermal components $\hat{\sigma}_t^\kappa$ characterise the rate-dependent interactions of dislocations with short-range obstacles that can be overcome with the assistance of thermal activation [2].

At different temperatures T and plastic strain rates $\dot{\varepsilon}$, the contributions to the flow stress σ_t^κ are related to their threshold counterparts $\hat{\sigma}_t^\kappa$ through the scaling functions $S_t^\kappa(\dot{\varepsilon}, T)$, so that

$$\sigma_t^\kappa = \hat{\sigma}_t^\kappa S_t^\kappa(\dot{\varepsilon}, T). \tag{2}$$

Considering the scaling relationship between the flow stress and theoretical threshold values of a material, σ_y can be expressed as

$$\frac{\sigma_y}{\mu} = \frac{\hat{\sigma}_a}{\mu} + \sum_\kappa \frac{\sigma_t^\kappa}{\mu} = \frac{\hat{\sigma}_a}{\mu} + \sum_\kappa S_t^\kappa(\dot{\varepsilon}, T)\frac{\hat{\sigma}_t^\kappa}{\mu_o}. \tag{3}$$

Here, μ_o is a reference value of the shear modulus μ, which is often modeled by [7]

$$\mu = \tilde{\mu}(T) = \mu_o - \frac{D_o}{\exp\left(\frac{T_o}{T}\right) - 1}, \tag{4}$$

in which T_o and D_o are empirical constants. The temperature dependence of μ is included in the scaling functions S_t^κ. The interaction kinetics for short-range obstacles are described using an Arrhenius expression while a phenomenological relation is used for the free energy function of stress [4].

The scaling functions $S_t^\kappa(\dot{\varepsilon}, T)$ now take the form

$$S_t^\kappa(\dot{\varepsilon}, T) = \left[1 - \left(\frac{kT}{g_{ot}^\kappa \mu b^3} \ln \frac{\dot{\varepsilon}_{ot}^\kappa}{\dot{\varepsilon}}\right)^{1/q_t^\kappa}\right]^{1/p_t^\kappa}, \tag{5}$$

where k is the Boltzmann constant, b is the magnitude of the Burger's vector, g_o is the normalized activation energy for dislocations to overcome the obstacles, $\dot{\varepsilon}_o$ is a constant and

p and q are statistical constants that characterize the shape of the obstacle profile ($0 \leq p \leq 1$, $1 \leq q \leq 2$) [4].

In the standard MTS model there are two thermal components, i.e. $\hat{\sigma}_t^{\kappa}$, $\kappa = 1, 2$. Using the notation $\hat{\sigma}_t^1 = \hat{\sigma}_i$ and $\hat{\sigma}_t^2 = \hat{\sigma}_\varepsilon$, the flow stress relation in (3) changes to

$$\frac{\sigma_y}{\mu} = \frac{\hat{\sigma}_a}{\mu} + S_i(\dot{\varepsilon}, T)\frac{\hat{\sigma}_i}{\mu_o} + S_\varepsilon(\dot{\varepsilon}, T)\frac{\hat{\sigma}_\varepsilon}{\mu_o}, \tag{6}$$

In (6), $\hat{\sigma}_i$ describes the thermal portion of the yield stress (non-evolving thermal stress component) and $\hat{\sigma}_\varepsilon$ describes the interaction of mobile dislocations with the forest dislocation structure (evolving component).

The evolution of $\hat{\sigma}_\varepsilon$ is given in rate form, by

$$\frac{d\hat{\sigma}_\varepsilon}{d\varepsilon} = \theta(T, \dot{\varepsilon}, \hat{\sigma}_\varepsilon) = \theta_o - \theta_r(T, \dot{\varepsilon}, \hat{\sigma}_\varepsilon), \tag{7}$$

where θ_o is the hardening due to dislocation accumulation (assumed constant) and θ_r is the dynamic recovery rate. The functional form of the hardening rate θ is chosen to fit experimental data. The tanh functional form [1], [2]

$$\theta = \theta_o \left(1 - \frac{\tanh\left[\frac{\alpha\hat{\sigma}_\varepsilon}{\hat{\sigma}_{\varepsilon s}}\right]}{\tanh(\alpha)} \right) \tag{8}$$

is used here although the power law form [5] is also a popular choice. The α parameter is a fitted constant and $\hat{\sigma}_{\varepsilon s}$ is the saturation threshold stress. θ_o assumes the role of the initial hardening rate. The hardening rate θ decreases with strain and reaches saturation. The saturation threshold stress $\hat{\sigma}_{\varepsilon s}$ is a function of both strain rate and temperature, through [1]

$$\ln \frac{\dot{\varepsilon}}{\dot{\varepsilon}_{\varepsilon so}} = \frac{g_{o\varepsilon s}\mu b^3}{kT} \ln \frac{\hat{\sigma}_{\varepsilon s}}{\hat{\sigma}_{\varepsilon so}} \tag{9}$$

where $\dot{\varepsilon}_{\varepsilon so}$, $g_{o\varepsilon s}$ and $\hat{\sigma}_{\varepsilon so}$ are empirically obtained constants.

II. Implementation into Abaqus

The MTS material model is implemented into an Abaqus UHARD user subroutine. This user subroutine is included in Section IV. The included subroutine can be used to calculate the yield stress (`SYIELD`) and gradients of yield stress with respect to equivalent plastic strain (`HARD(1)`) and equivalent plastic strain rate (`HARD(2)`). The UHARD subroutine only takes care of the plastic response and the user should still account for the temperature dependence of the elastic response.

A limitation in the implemented subroutine is that the mechanical threshold scaling functions in (5) are calculated for a plastic strain rate above 10^{-8}. The subroutine can therefore not distinguish between plastic strain rates below this arbitrarily selected threshold value. The gradients with respect to equivalent plastic strain and equivalent plastic strain rate (`HARD(1)` $= \frac{\partial \sigma_y}{\partial \varepsilon_p}$ and `HARD(2)` $= \frac{\partial \sigma_y}{\partial \dot{\varepsilon}_p}$) are evaluated analytically to allow quadratic convergence.

The MTS UHARD user subroutine requires 19 material parameters and 8 state dependent variables. The definition of these material parameters and state dependent variables are given in Table I. In the subsections to follow, the paper will cover the calculation of the evolving thermal stress component and analytical gradients as well as how and why the state dependent variables are used.

TABLE I
Abaqus and MTS UHARD subroutine material property definition.

Variable	Equations	UHARD	ABAQUS
μ_o	(4)	`ZMU0`	`PROPS(1)`
D_o	(4)	`D0`	`PROPS(2)`
T_o	(4)	`TEMP0`	`PROPS(3)`
$\hat{\sigma}_a$	(1), (3), (6)	`SA`	`PROPS(4)`
$\hat{\sigma}_i$	(6)	`SI`	`PROPS(5)`
$\hat{\sigma}_\varepsilon$	(6), (7), (8)	`SE0`	`PROPS(6)`
$\hat{\sigma}_{\varepsilon so}$	(9)	`SES0`	`PROPS(7)`
θ_o	(7), (8)	`TH0`	`PROPS(8)`
$^k/_{b^3}$	(5), (9)	`ZKB3`	`PROPS(9)`
α	(8)	`ALPHA`	`PROPS(10)`
g_{oi}	(5)	`G0I`	`PROPS(11)`
$g_{o\varepsilon}$	(5)	`G0E`	`PROPS(12)`
$g_{o\varepsilon s}$	(9)	`G0ES`	`PROPS(13)`
$\dot{\varepsilon}_o$	(5)	`ER0`	`PROPS(14)`
$\dot{\varepsilon}_{\varepsilon so}$	(9)	`ER0ES`	`PROPS(15)`
q_i	(5)	`QI`	`PROPS(16)`
p_i	(5)	`PI`	`PROPS(17)`
q_ε	(5)	`QE`	`PROPS(18)`
p_ε	(5)	`PE`	`PROPS(19)`

A. Calculating the evolving thermal component

Midpoint integration is used to determine the value of the evolving thermal stress component ($\hat{\sigma}_\varepsilon$) at the end of a specific time step. The plastic strain rate, duration of the time increment and change in temperature over the time increment are taken into account. The value of the evolving thermal stress component at time t^{n+1} is now given by

$$\begin{aligned}\hat{\sigma}_\varepsilon^{n+1} &= \hat{\sigma}_\varepsilon^n + \frac{\triangle\varepsilon_p}{2}\left(\theta(T^n, \dot{\varepsilon}^n, \hat{\sigma}_\varepsilon^n) + \theta(T^{n+1}, \dot{\varepsilon}^{n+1}, \hat{\sigma}_\varepsilon^{n+1})\right) \\ &= \hat{\sigma}_\varepsilon^n + \frac{\triangle\varepsilon_p}{2}\left(\theta^n + \theta^{n+1}\right).\end{aligned} \tag{10}$$

The choice of the tanh functional form and midpoint integration require solution by the Newton-Raphson method. In the Abaqus UHARD implementation, an initial guess is assigned $\hat{\sigma}_\varepsilon^{n+1} = \hat{\sigma}_\varepsilon^n$. The update of $\hat{\sigma}_\varepsilon^{n+1}$ is then performed iteratively by the Newton-Raphson method:

$$\left(\hat{\sigma}_\varepsilon^{n+1}\right)_{i+1} = \left(\hat{\sigma}_\varepsilon^{n+1}\right)_i - \frac{\left(f(\hat{\sigma}_\varepsilon^{n+1})\right)_i}{\left(f'(\hat{\sigma}_\varepsilon^{n+1})\right)_i}. \tag{11}$$

Equation (11) is iterated to convergence for a fixed timestep at a specific element integration point, where

$$f(\hat{\sigma}_\varepsilon^{n+1}) = \hat{\sigma}_\varepsilon^{n+1} - \hat{\sigma}_\varepsilon^n - \frac{\triangle\varepsilon_p}{2}\left(\theta^n + \theta^{n+1}\right)$$

and

$$f'(\hat{\sigma}_\varepsilon^{n+1}) = 1 - \frac{\triangle\varepsilon_p}{2}\frac{d\theta^{n+1}}{d\hat{\sigma}_\varepsilon^{n+1}}.$$

For the tanh functional form in (8),

$$\theta^{n+1} = \theta_o \left[1 - \frac{\tanh\left(\frac{\alpha \hat{\sigma}_\varepsilon^{n+1}}{\hat{\sigma}_{\varepsilon s}^{n+1}}\right)}{\tanh(\alpha)} \right], \tag{12}$$

and hence

$$\frac{d\theta^{n+1}}{d\hat{\sigma}_\varepsilon^{n+1}} = \frac{-\alpha\theta_o}{\hat{\sigma}_{\varepsilon s}^{n+1} \tanh(\alpha) \cosh^2\left(\frac{\alpha \hat{\sigma}_\varepsilon^{n+1}}{\hat{\sigma}_{\varepsilon s}^{n+1}}\right)}. \tag{13}$$

B. Analytical gradients

The partial derivatives `HARD(1)` and `HARD(2)` are evaluated analytically to allow quadratic convergence of the displacement solution. These gradients represent the change in the calculated `SYIELD` for a different `EQPLAS` and `EQPLASRT` input respectively.

Using the general MTS definition in (6), the yield stress at the end of the current increment, σ_y^{n+1}, is

$$\sigma_y^{n+1} = \hat{\sigma}_a + \frac{\mu^{n+1}}{\mu_o}\left(S_i^{n+1}\hat{\sigma}_i + S_\varepsilon^{n+1}\hat{\sigma}_\varepsilon^{n+1}\right). \tag{14}$$

The first partial derivative with respect to $\texttt{EQPLAS} = \varepsilon_p^{n+1}$ is determined analytically by

$$\texttt{HARD(1)} = \frac{\partial \sigma_y^{n+1}}{\partial \varepsilon_p^{n+1}} = \frac{\mu^{n+1}}{\mu_o}\left(S_\varepsilon^{n+1}\frac{d\hat{\sigma}_\varepsilon^{n+1}}{d\varepsilon_p^{n+1}}\right). \tag{15}$$

Given the midpoint evaluation of $\hat{\sigma}_\varepsilon^{n+1}$ in (10), the tanh functional form of the hardening rate from (12) and an equivalent plastic strain update $\triangle\varepsilon_p = \varepsilon_p^{n+1} - \varepsilon_p^n$:

$$\frac{d\hat{\sigma}_\varepsilon^{n+1}}{d\varepsilon_p^{n+1}} = \frac{\theta^n + \theta^{n+1}}{2} + \frac{\triangle\varepsilon_p}{2}\frac{d\theta^{n+1}}{d\varepsilon_p^{n+1}}. \tag{16}$$

Now, using (13) and the chain rule

$$\frac{d\theta^{n+1}}{d\varepsilon_p^{n+1}} = \frac{d\theta^{n+1}}{d\hat{\sigma}_\varepsilon^{n+1}}\frac{d\hat{\sigma}_\varepsilon^{n+1}}{d\varepsilon_p^{n+1}}, \tag{17}$$

the partial derivative with respect to the equivalent plastic strain `HARD(1)` is determined by

$$\texttt{HARD(1)} = \frac{\partial \sigma_y^{n+1}}{\partial \varepsilon_p^{n+1}} = \frac{\mu^{n+1} S_\varepsilon^{n+1}(\theta^n + \theta^{n+1})}{2\mu_o(1-A)}; \tag{18}$$

$$A = \frac{\triangle\varepsilon_p}{2}\frac{d\theta^{n+1}}{d\hat{\sigma}_\varepsilon^{n+1}}.$$

Similarly, the second partial derivative with respect to $\texttt{EQPLASRT} = \dot{\varepsilon}_p^{n+1}$ is determined from

$$\begin{aligned}\texttt{HARD(2)} &= \frac{\partial \sigma_y^{n+1}}{\partial \dot{\varepsilon}_p^{n+1}} \\ &= \frac{\mu^{n+1}}{\mu_o}\left(\frac{dS_i^{n+1}}{d\dot{\varepsilon}_p^{n+1}}\hat{\sigma}_i + \frac{dS_\varepsilon^{n+1}}{d\dot{\varepsilon}_p^{n+1}}\hat{\sigma}_\varepsilon^{n+1} + S_\varepsilon^{n+1}\frac{d\hat{\sigma}_\varepsilon^{n+1}}{d\dot{\varepsilon}_p^{n+1}}\right).\end{aligned} \tag{19}$$

Using the Arrhenius expression for the scaling functions in (5), the partial derivatives of the scaling functions with respect to the equivalent plastic strain rate can be determined from

$$\begin{aligned}\frac{d(S_t^\kappa)^{n+1}}{d\dot{\varepsilon}_p^{n+1}} &= \frac{\gamma_t^\kappa}{p_t^\kappa q_t^\kappa \dot{\varepsilon}_p^{n+1}}\left[1 - \left(\gamma_t^\kappa \ln\left(\frac{\dot{\varepsilon}_{ot}^\kappa}{\dot{\varepsilon}_p^{n+1}}\right)\right)^{\frac{1}{q_t^\kappa}}\right]^{\frac{1-p_t^\kappa}{p_t^\kappa}} \\ &\times \left(\gamma_t^\kappa \ln\left(\frac{\dot{\varepsilon}_{ot}^\kappa}{\dot{\varepsilon}_p^{n+1}}\right)\right)^{\frac{1-q_t^\kappa}{q_t^\kappa}};\end{aligned} \tag{20}$$

$$\gamma_t^\kappa = \frac{kT^{n+1}}{g_{ot}^\kappa \mu^{n+1} b^3}.$$

Using (9), the midpoint evaluation of $\hat{\sigma}_\varepsilon^{n+1}$ in (10), the chain rule

$$\frac{d\theta^{n+1}}{d\dot{\varepsilon}_p^{n+1}} = \frac{d\theta^{n+1}}{d\hat{\sigma}_\varepsilon^{n+1}}\frac{d\hat{\sigma}_\varepsilon^{n+1}}{d\dot{\varepsilon}_p^{n+1}} \tag{21}$$

and the tanh functional form of the hardening rate from (12),

$$\frac{d\hat{\sigma}_\varepsilon^{n+1}}{d\dot{\varepsilon}_p^{n+1}} = \frac{A}{(A-1)}\frac{\gamma_{\varepsilon s}\hat{\sigma}_{\varepsilon so}\hat{\sigma}_\varepsilon^{n+1}}{\dot{\varepsilon}_{o\varepsilon s}\hat{\sigma}_{\varepsilon s}^{n+1}}\left(\frac{\dot{\varepsilon}_p^{n+1}}{\dot{\varepsilon}_{o\varepsilon s}}\right)^{\gamma_{\varepsilon s}-1}; \tag{22}$$

$$\gamma_{\varepsilon s} = \frac{kT^{n+1}}{g_{o\varepsilon s}\mu^{n+1}b^3}; \quad A = \frac{\triangle\varepsilon_p}{2}\frac{d\theta^{n+1}}{d\hat{\sigma}_\varepsilon^{n+1}}.$$

In order to evaluate `HARD(2)` analytically, (20) and (22) are determined first and then simply substituted into (19).

C. State dependent variables

The implemented user subroutine makes use of 8 state dependent variables. The first state dependent variable, `STATEV(1)` stores the value of the evolving thermal stress component $\hat{\sigma}_\varepsilon^n$ at the end of the previous increment. `STATEV(2)` stores the current update in the evolving thermal stress component, $\triangle\hat{\sigma}_\varepsilon^{n+1}$. In order to evaluate θ^n and so properly use midpoint integration in (10) for example, the equivalent plastic strain as well as the equivalent plastic strain rate at the end of

TABLE II
MTS UHARD STATE DEPENDENT VARIABLE DEFINITION AND ALLOCATION.

Variable	Definition	Allocation
$\hat{\sigma}_\varepsilon^n$	$\hat{\sigma}_\varepsilon$ at time t^n, the start of the current increment.	`STATEV(1)`
$\triangle\hat{\sigma}_\varepsilon^{n+1}$	Change in $\hat{\sigma}_\varepsilon$ for current increment.	`STATEV(2)`
${\varepsilon_p}^n$	Equivalent plastic strain ε_p at the end of the previous increment.	`STATEV(3)`
${\varepsilon_p}^{n+1}$	Equivalent plastic strain ε_p at the end of the current increment.	`STATEV(4)`
$\dot{\varepsilon_p}^n$	Equivalent plastic strain rate $\dot{\varepsilon_p}$ at the end of the previous increment.	`STATEV(5)`
$\dot{\varepsilon_p}^{n+1}$	Equivalent plastic strain rate ε_p at the end of the current increment.	`STATEV(6)`
`KINC`	`KINC` verification counter allowing a single update of the relevant variables	`STATEV(7)`
`KSTEP`	`KSTEP` verification counter used to reset `STATEV(7)` should the analysis move on to a different step.	`STATEV(8)`

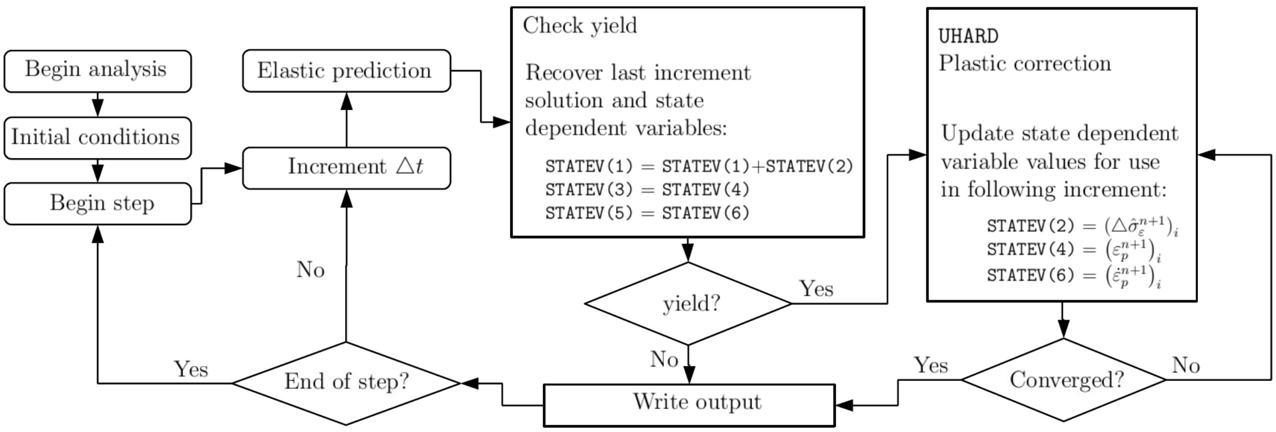

Fig. 1. Flow chart of Abaqus process indicating state variables used in the UHARD user subroutine. After an increment has converged, values of the state dependent variables `STATEV(2)`, `STATEV(4)` and `STATEV(6)` can be updated to state dependent variables `STATEV(1)`, `STATEV(3)` and `STATEV(5)` for use in the next solution increment.

the previous increment is required. `STATEV(3)` and `STATEV(5` are used to store these values of ε_p^n and $\dot{\varepsilon}_p^n$.

Since multiple calls to the user hardening subroutine ar required for convergence, it is imperative that the evolvin thermal stress component as well as the equivalent plasti strain and equivalent plastic strain rate are only stored i `STATEV(1)`, `STATEV(3)` and `STATEV(5)` for use in the nex increment once a converged solution is obtained. The stat dependent variable `STATEV(7)` is used to ensure that these stat dependent variables are only updated for the first UHARI subroutine evaluation in a specific increment. These update therefore take place when the yield condition is checked usin the state dependent variable values at the end of the previous converged solution.

The state dependent variable updates are as follow:

- The converged value of the evolving thermal stress component update $\triangle\hat{\sigma}_\varepsilon$ for a previous increment stored in `STATEV(2)` is added to `STATEV(1)`.
- `STATEV(3)` is updated to contain the converged value of `EQPLAS` for the previous increment stored in `STATEV(4)`.
- `STATEV(5)` is updated to contain the converged value of `EQPLASRT` for the previous increment stored in `STATEV(6)`.

`STATEV(8)` is used to reset the increment counter `STATEV(7)` to 0 if the simulation moves on to another step. The definition and allocation of the state dependent variables is also given in Table II, with a flow chart of the Abaqus solution procedure and state dependent variable updates visible in Figure 1.

III. Examples

As an example of the MTS model performance, the model parameters are calibrated using isothermal, constant strain rate data on OFHC Cu digitised from the Ph.D. thesis by A.B. Tanner [6]. The Johnson-Cook plasticity model [3] is calibrated on the same data. In the Johnson-Cook plasticity model, the

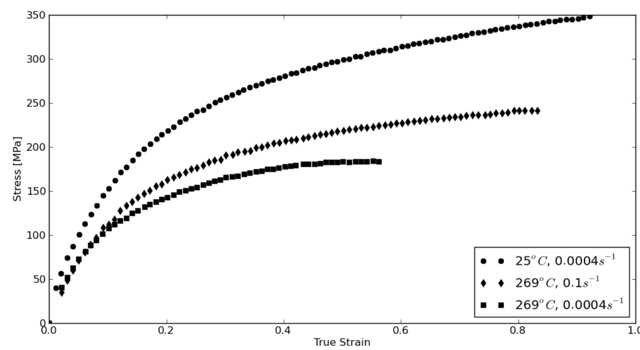

Fig. 2. Isothermal constant strain rate stress-strain data for OFHC Copper in compression as digitised from [6].

flow stress is given by the closed form expression [3]

$$\sigma_y = \left(\sigma_0 + B\varepsilon_p^n\right)\left(1 + C\ln\frac{\dot{\varepsilon}_p}{\dot{\varepsilon}_0}\right)\left(1 - \left[\frac{T - T_r}{T_m - T_r}\right]^m\right). \tag{23}$$

The data digitised from the Ph.D. of A.B. Tanner is visible in Figure 2. These stress-strain curves are of compression data on OFHC copper at:

- a temperature of 25^{o}C and strain rate of $0.0004s^{-1}$;
- a temperature of 269^{o}C and strain rate of $0.1s^{-1}$ and
- a temperature of 269^{o}C and strain rate of $0.0004s^{-1}$.

The model implemented and discussed in this article is incapable of describing recrystalisation or material softening. For this reason, the stress-strain data at 269^{o}C and strain rate of $0.0004s^{-1}$ was only used up to a true strain of approximately 55%.

The elastic properties of the material was chosen as that descibed in [6]. For consistency, both MTS and Johnson-Cook models use the shear modulus relation

$$\mu = 1000\left[47.093 - \left(0.1429 + 0.0002763T^2\right)^{0.5}\right] \tag{24}$$

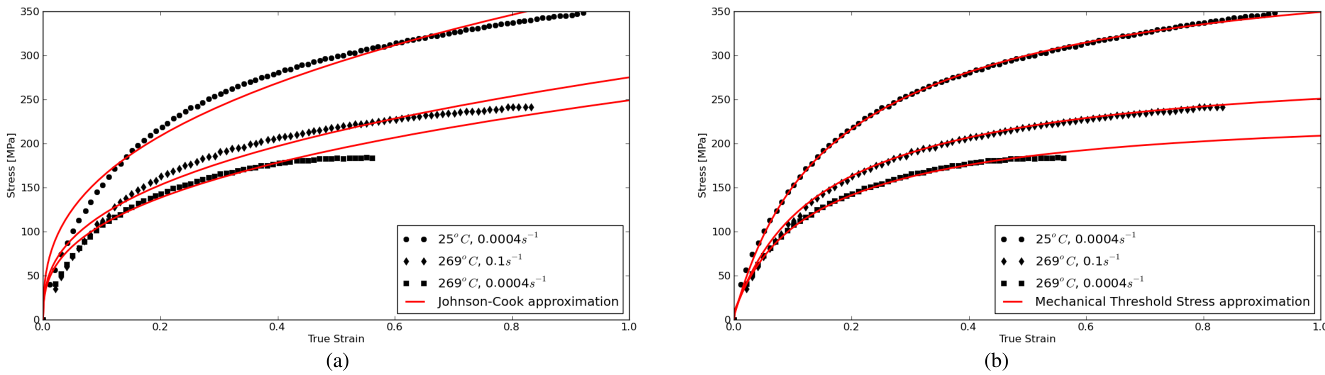

Fig. 3. Tuned (a) Johnson-Cook and (b) Mechanical Threshold Stress material models for isothermal, constant strain rate compression data.

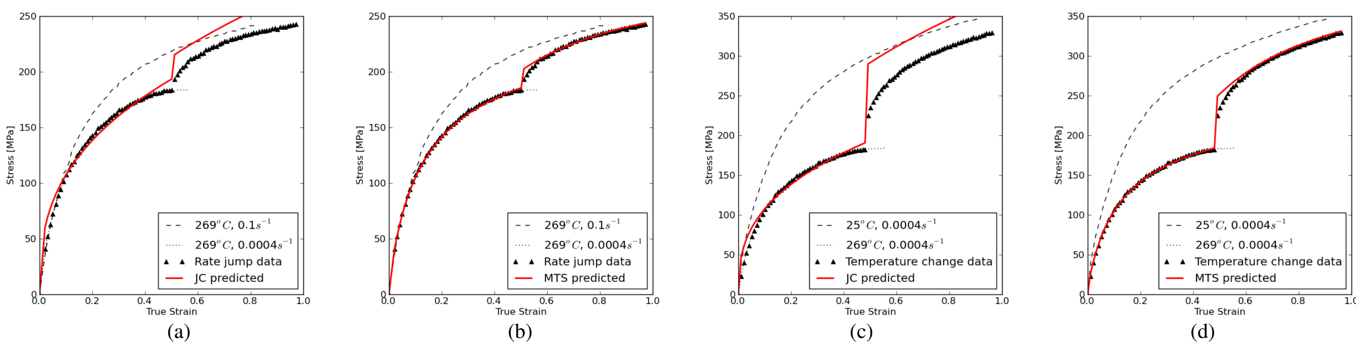

Fig. 4. Comparison of Johson-Cook and MTS calculated response compared to experimental data of a strain rate jump test and temperature change test after 50% compression. (a) Johnson-Cook and (b) MTS result compared to the strain rate jump test data of [6]. (c) Johnson-Cook and (d) MTS result compared to the temperature change test data of [6].

instead of the relationship in (4). Using $\nu = {}^{1}/{}_{3}$ [6], the elastic modulus is obtained from the shear modulus by using

$$E = 2\mu(1+\nu). \tag{25}$$

An initial estimate on the model parameter values were obtained in [6]. An optimisation routine is then run to calibrate the relevant parameters by comparing the numerical stress-strain response to the isothermal, constant strain rate data visible in Figure 2. For the MTS model calibration, the parameters $\hat{\sigma}_a$, $\hat{\sigma}_i$, $\hat{\sigma}_{\varepsilon so}$, θ_o, α, g_{oi}, $g_{o\varepsilon}$ and $g_{o\varepsilon s}$ were tuned using this optimisation procedure. The Johnson-Cook model parameters σ_0, B, n, C and m were tuned in the same way.

The material model parameter values for both plasticity models are visible in Table III. The curve fits that result in the best match with the experimental data is displayed in Figure 3(a) for the Johnson-Cook model and in Figure 3(b) for the Mechanical Threshold stress model. In these figures it is visible that the physically based MTS model (initially developed specifically for Copper) is better suited to replicate the isothermal constant strain rate OFHC Cu data.

Two additional experimental data sets were also digitised from [6]. In the first experiment, the specimen was kept at 269^{o}C. It is first compressed up to 50% strain at a constant strain rate of $0.0004s^{-1}$ and then at a constant strain rate of $0.1s^{-1}$. Using the Johnson-Cook and MTS models with the material model parameter values in Table III and elastic response in (24) and (25), the experimental strain and strain rate history is fed into the material models resulting in Figure 4(a) for the Johnson-Cook model and Figure 4(b) for the MTS model respectively.

TABLE III
MTS AND JC MATERIAL PROPERTY VALUES CALIBRATED ON DATA.

MTS		JC	
Variable	Value	Variable	Value
T_o	208	σ_0	0.0104
$\hat{\sigma}_a$	1.635	B	419.67
$\hat{\sigma}_i$	0.324	n	0.364
$\hat{\sigma}_\varepsilon$	0	C	0.0195
$\hat{\sigma}_{\varepsilon so}$	412.12	$\dot{\varepsilon}_0$	0.0001
θ_o	2026.83	T_r	208
${}^{k}/{}_{b^3}$	0.848	T_m	1070
α	1.799	m	0.91
g_{oi}	0.027		
$g_{o\varepsilon}$	1.313		
$g_{o\varepsilon s}$	0.553		
$\dot{\varepsilon}_o$	$1e^7$		
$\dot{\varepsilon}_{\varepsilon so}$	$1e^7$		
q_i	1.5		
p_i	0.5		
q_ε	1		
p_ε	0.6667		

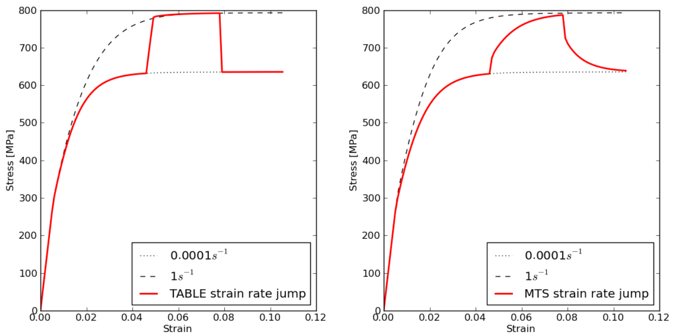

(a) (b)

Fig. 5. Comparison of (a) Table based method and (b) Abaqus MTS UHARD subroutine for a strain rate jump test.

In the second experiment, the test was carried out at a constant strain rate of $0.0004s^{-1}$. The specimen is kept at 269^{o}C up to 50% strain and then cooled down to 25^{o}C before compressing the specimen further. The result of the Johnson-Cook model is visible in Figure 4(c) with the result of the MTS model visible in Figure 4(d).

The Johnson-Cook model consists of a closed form expression and the change in strain rate or temperature simply translates into a jump from one curve to another. This simple jump between curves would be true for any model that describes the relationship between stress and strain subject to strain rate and temperature dependence in a closed form expression.

Figure 5 illustrates the difference in the results of a strain rate jump test example if done using the UHARD and table based methods in Abaqus. This is to illustrate what happens when using the table based method in Abaqus versus the user hardening subroutine.

Given a selection of MTS material parameters and strain rate dependent tables, the black lines in Figures 5(a) and (b) are recovered if a single element is compressed 10% in a $1000s$ and $0.1s$ period respectively. These curves are the reference curves for a strain rate of $0.0001s^{-1}$ and $1s^{-1}$. In the strain rate jump test, the element is first compressed 4.5% in a $400s$ period, it is then compressed an additional 3% in a $0.03s$ period and finally an additional 2.5% in $250s$. The results of these simulations are visible as the red lines in Figure 5.

As with the closed form expression of the Johnson-Cook model, the table based method simply interpolates between the curves it was provided with. Although it is therefore possible to replicate the isothermal, constant strain rate experimental data of Figure 2 given the correct table of yield stress versus plastic strain and plastic strain rate for example, the physically observed effect of plastic history would not be captured in the temperature change or strain rate jump tests when using the table based method.

The state dependent update of the thermally influenced evolving stress component allows a physically observed change in the stress state which is not only influenced by temperature and strain rate. The modelled material response is clearly also dependent on the plastic history.

IV. MTS USER HARDENING SUBROUTINE

```
      SUBROUTINE UHARD(SYIELD,HARD,EQPLAS,EQPLASRT,
     $ TIME,DTIME,TEMP,DTEMP,NOEL,NPT,LAYER,KSPT,
     $ KSTEP,KINC,CMNAME,NSTATV,STATEV,NUMFIELDV,
     $ PREDEF,DPRED,NUMPROPS,PROPS)
C
      IMPLICIT REAL*8(A-H,O-Z)
      PARAMETER (NPRECD=2)
C
      CHARACTER*80 CMNAME
      DIMENSION HARD(3),STATEV(NSTATV),TIME(*),
     $ PREDEF(NUMFIELDV),DPRED(*),PROPS(*)
C
      ZMU0   = PROPS(1)
      D0     = PROPS(2)
      TEMP0  = PROPS(3)
      SA     = PROPS(4)
      SI     = PROPS(5)
      SE0    = PROPS(6)
      SES0   = PROPS(7)
      TH0    = PROPS(8)
      ZKB3   = PROPS(9)
      ALPHA  = PROPS(10)
      G0I    = PROPS(11)
      G0E    = PROPS(12)
      G0ES   = PROPS(13)
      ER0    = PROPS(14)
      ER0ES  = PROPS(15)
      QI     = PROPS(16)
      PI     = PROPS(17)
      QE     = PROPS(18)
      PE     = PROPS(19)
      T_A    = TEMP
      T_B    = TEMP+DTEMP
C
C INITIALIZE EVOLVING STATE VARIABLE
C
      IF(KSTEP.EQ.1.AND.KINC.EQ.1)THEN
        STATEV(1)  = SE0
        STATEV(6)  = 1.E-8
      ENDIF
C
C CHECK IF THE ANALYSIS HAS MOVED ON TO NEW STEP
C AND INITIALIZE COUNTER STATEV(7)
C
      IF(STATEV(8).LT.KSTEP)THEN
        STATEV(8)  = KSTEP
        STATEV(7)  = 0.
      ENDIF
C
C SET EVOLVING STATE VARIABLE FROM UPDATE
C EVALUATED IN PREVIOUS INCREMENT
C
      IF(STATEV(7).LT.KINC)THEN
        STATEV(1)  = STATEV(1)+STATEV(2)
        STATEV(3)  = STATEV(4)
        STATEV(5)  = STATEV(6)
        STATEV(7)  = KINC
      ENDIF
C
C SET VALUE OF SE AT BEGINNIG OF INCREMENT FROM
C STATE VARIABLE AT END OF PREVIOUS
C
      SE = STATEV(1)
C
C DETERMINE INITIAL INCREMENT TEMPERATURE EFFECT
C ON VARIABLE ZMU
C
```

```
      IF(T_A.EQ.0.D0)THEN
C
C USE THRESHOLD VALUE. (SCALE FACTOR = 1)
C
        ZMU_A = ZMU0
      ELSE
C
C DETERMINE ZMU USING TEMPERATURE SCALE FACTOR
C
        ZMU_A = ZMU0-D0/(EXP(TEMP0/T_A)-1.D0)
      ENDIF
C
C DETERMINE FINAL INCREMENT TEMPERATURE EFFECT
C ON VARIABLE ZMU
C
      IF(T_B.EQ.0.D0)THEN
C
C USE THRESHOLD VALUE. (SCALE FACTOR = 1)
C
        ZMU_B = ZMU0
      ELSE
C
C DETERMINE ZMU USING TEMPERATURE SCALE FACTOR
C
        ZMU_B = ZMU0-D0/(EXP(TEMP0/T_B)-1.D0)
      ENDIF
C
C DETERMINE SCALING FACTORS, YIELD STRESS AND
C STATE VARIABLE EVOLUTION ACCORDING TO
C MECHANICAL THRESHOLD STRESS MATERIAL MODEL:
C   CHECK PLASTIC DEFORMATION RATE IS HIGHER
C   THAN TOLERANCE
C
      IF(EQPLASRT.LE.1.E-8)THEN
        RATEB = 1.E-8
      ELSE
        RATEB = EQPLASRT
      ENDIF
C
C DETERMINE CHANGE IN PLASTIC DEFORMATION
C
      DEPSP = EQPLAS - STATEV(3)
      STATEV(4) = EQPLAS
      RATEA = STATEV(5)
      STATEV(6) = RATEB
C
C CALCULATE LUMPED EQUATION CONSTANTS
C
      SFE0 = ZKB3*T_B/(G0E*ZMU_B)
      SFE1 = SFE0*LOG(ER0/RATEB)
      SFE2 = 1.D0-(SFE1**(1.D0/QE))
      SFI0 = ZKB3*T_B/(G0I*ZMU_B)
      SFI1 = SFI0*LOG(ER0/RATEB)
      SFI2 = 1.D0-(SFI1**(1.D0/QI))
      ZKESA = ZKB3*T_A/(G0ES*ZMU_A)
      ZKESB = ZKB3*T_B/(G0ES*ZMU_B)
C
C CALCULATE SCALE FUNCTIONS
C
      SFE = SFE2**(1.D0/PE)
      SFI = SFI2**(1.D0/PI)
      SESA = SES0*((RATEA/ER0ES)**ZKESA)
      SESB = SES0*((RATEB/ER0ES)**ZKESB)
C
C DETERMINE EVOLUTION AND STRAIN
C
      SE_B = SE; FS = 1.;COUNTER = 0
      HARD_A = TH0*(1.-(TANH(ALPHA*SE/SESA)
     .        /TANH(ALPHA)))
C
C NEWTON-RAPHSON UP TO CONVERGENCE OR
C 100 ITERATIONS
C
      DO WHILE ((ABS(FS).GT.1.E-8).AND.
     .        (COUNTER.LT.100))
        COUNTER = COUNTER + 1
        HARD_B = TH0*(1.0-(TANH(ALPHA*SE_B/SESB)
     .        /TANH(ALPHA)))
        DFS0 = DEPSP*TH0*ALPHA/(TANH(ALPHA)
     .        *SESB*COSH(ALPHA*SE_B/SESB)**2)
        FS = SE_B-SE-DEPSP*(HARD_A+HARD_B)/2.
        DFS = 1.+DFS0/2.
        SE_B = SE_B - FS/DFS
      END DO
      HARD_B = TH0*(1.0-(TANH(ALPHA*SE_B/SESB)
     .        /TANH(ALPHA)))
      SE_UPD = SE_B-SE
C
C DETERMINE SYIELD CONSIDERING THE UPDATE ON SE
C
      SYIELD = SA+(SFE*SE_B+SFI*SI)*(ZMU_B/ZMU0)
C
C SAVE CURRENT VALUE OF STATE VARIABLE UPDATE IN
C STATEV(2)
C
      STATEV(2) = SE_UPD
C
C DERIVATIVES OF SYIELD W.R.T D_EPSP, D_EPSRATE
C AND D_TEMPERATURE
C
      DSFE0 = (SFE2**(1.D0/PE - 1.D0))/(PE*QE*RATEB)
      DSFE = SFE0*(SFE1**(1.D0/QE - 1.D0))*DSFE0
      DSFI0 = (SFI2**(1.D0/PI - 1.D0))/(PI*QI*RATEB)
      DSFI = SFI0*(SFI1**(1.D0/QI - 1.D0))*DSFI0
C
C D(SES)/D_ERATE
C
      DSES = ZKESB*SES0*((RATEB/ER0ES)**(ZKESB-
     .       1.D0))/ER0ES
      DFS0 = DEPSP*TH0*ALPHA/(2*TANH(ALPHA)
     .       *SESB*COSH(ALPHA*SE_B/SESB)**2)
      DSE = DFS0*SE_B*DSES/(SESB*(1.+DFS0))
C
C HARD(1) = D(SYIELD)/D(EQPLAS)
C
      HARD(1) = SFE*ZMU_B*(HARD_A+HARD_B)/(2.*ZMU0
     .        *(1+DFS0))
C
C HARD(2) = D(SYIELD)/D(EQPLASRT)
C
      HARD(2) = ZMU_B*((DSFI*SI)+(DSFE*SE_B)
     .        +(SFE*DSE))/ZMU0
      RETURN
      END
```

V. Conclusion

In this paper, the Mechanical Threshold Stress model was implemented into an Abaqus UHARD user subroutine. This user subroutine is also provided in the paper. The use of state dependent variables is explained and analytical partial derivatives are provided so that the solution is obtained quadratically.

In the examples on real experimental data, the benefit of having a physical, state variable based plasticity model instead of a closed form expression or table based plasticity definition is evident. In applications where the evolution of the yield stress is required as a function of the plastic history, the MTS plasticity model included in the paper can be used with little additional effort.

References

[1] Chen, S.R., Gray, G.T., 1996. Constitutive Behaviour of Tantalum and Tantalum-Tungsten Alloys. Metall and Mat Trans 27(A), 2994-3006.

[2] Follansbee, P.S., Kocks, U.F., 1988. A Constitutive Description of Copper Based on the Use of the Mechanical Threshold Stress as an Internal State Variable. Acta Metall 36, 81-93.
[3] Johnson, G.R. and Cook, W.H., 1983, A Constitutive Model and Data for Metals Subjected to Large Strains, High Strain Rates and High Temperatures, in: Proceedings of Seventh International Symposium on Ballistics, The Hague, 541-547.
[4] Kocks, U.F., Argon, A.S., Ashby, M.F., 1975. Thermodynamics and Kinetics of Slip. In: Progress in Materials Science 19, Pergamon Press, New York.
[5] Kocks, U.F., Tomé, C.N., Wenk, H.R., 1998. Texture and Anisotropy. Cambridge University Press.
[6] Tanner, A.B., 1998. Modeling temparature and strain rate history effects in OFHC Cu., Ph.D. Thesis., Georgia Institute of Technology.
[7] Varshni, Y.P., 1970. Temperature Dependence of the Elastic Constants. Phys Rev B 2, 3952-3958.